4th International Symposium on Virtual Reality, Archaeology and Intelligent Cultural Heritage
(VAST 2003)
D. Arnold, A. Chalmers, F. Niccolucci (Editors)

Virtual Vessel Reconstruction from a Fragment's Profile

M. Kampel[+] and F. J. Melero [*]

[+]Vienna University of Technology,
Institute of Computer Aided Automation,
Pattern Recognition and Image Processing Group
Favoritenstr. 9, 183-2, A-1040 Vienna
kampel@prip.tuwien.ac.at

[*]Universidad de Granada,
E.T.S. Ingeniería Informática,
Dpt. Lenguajes y Sistemas Informáticos,
C/. Daniel Saucedo Aranda s/n, E-18071 Granada, Spain
fjmelero@ugr.es

Abstract

Every archaeological excavation must deal with a vast number of ceramic fragments. The documentation, administration and scientific processing of these fragments represent a temporal, personnel, and financial problem. Up to now documentation and classification have been done manually which means a lot of routine work for archaeologists and a very inconsistent representation of the real object. First, there may be errors in the measuring process (diameter or height may be inaccurate). Second, the drawing of the fragment should be in a consistent style, which is not possible since a drawing of an object without interpreting it is very hard to do.

We are developing a documentation system for archaeological fragments based on their profile, which is the cross-section of the fragment in the direction of the rotational axis of symmetry. Hence the position of a fragment (orientation) on a vessel is important, since it allows a good profile to be obtained.

This paper presents two different approaches to the estimation of the orientation of archaeological fragments and the profile extraction. One method is based on a Hough inspired approach and the other is based on genetic algorithms and expert interaction. We compare the methods and show results with respect to robustness, applicability, and accuracy.

1. Introduction

Ceramics are one of the most widespread archaeological finds and are a short-lived material. This property helps researchers to document changes of style and ornaments. Therefore, ceramics are used to distinguish between chronological and ethnic groups. Furthermore, ceramics are used in economic history to show trading routes and cultural relationships [15]. In particular ceramic vessels, where shape and decoration are exposed to constantly changing fashion, not only allow a basis for dating the archaeological strata, but also provide evidence of local production and trade relations of a community as well as the consumer behaviour of the local population [15].

The documentation, administration and scientific processing of these fragments represents a temporal, personnel and financial problem [6]. Various excavation projects have been completed many years ago, but due to these problems their findings have yet to be published (see [9]). Scientific evaluation in archaeological practice often suffers due to extensive amounts of time required for the documentation and classification of ceramic finds [15]. Many publications do little more than present the drawings, descriptions and determinations of the objects found [22]. Thus it is frequently the case that several hundred pages of catalogues and illustrations are accompanied by only a few pages of analysis [7].

Figure 1: *Boxes filled with ceramics stored in archives.*

Figure 1 shows boxes filled with ceramics stored in an archive. If one asks archaeologists what they use pottery for (or why excavated fragments of pottery are kept) they will probably reply 'for dating evidence'. This dating evidence furthermore splits into three different types of evidence that is obtained from excavated pottery or its fragments [15]:

- Dating
- Distribution relating to trade
- Function and/or status

These are based on the fact that every pot was made or used at a certain time, made at a certain place, and used for a certain purpose. Therefore, every fragment or pot holds the information about when, where, and what it was made for. This fact places a heavy burden on excavators and primary processors or recorders of the material since the primary task of pottery research is comparison [15]. This means that pottery must be grouped and recorded in a way that facilitates a comparison.

In Section 2 we describe the manual process of archaeological documentation. In order to find the correct orientation and profile automatically we developed an approach for finding the axis of rotation of the fragment, and then extract the profile section, which is described in Section 3. Additionally, we present an approach that follows the traditional archaeological methodology steps, based on estimating the orientation by computing a so called orifice plane of the fragment in a semi automatic way, which is explained in Section 4. Each method was separately developed by the authors. Together, the synergy arising from both these approaches will lend considerable benefit to the automated archivation of archaeological fragments and serve the needs of the archaeological community. Results and a comparison of the two approaches are given in Section 5.

2. Traditional archaeological documentation and reconstruction

Traditional archaeological documentation and reconstruction is based on the so-called profile of the object, which is the cross-section of the fragment in the direction of the rotational axis of symmetry. This two-dimensional plot holds all the information needed to perform archaeological research. The correct profile and the correct axis of rotation are thus essential to reconstruct and classify archaeological ceramics. Figure 2 shows the inner side of a fragment on the left and its left side (broken surface) on the middle, and the profile section on the right.

(a) (b) (c)

Figure 2: *(a) Archaeological fragment (b) site of fracture (c) profile section.*

The recording of fragments consists of:

1. Photographing
2. Measuring
3. Drawing
4. Grouping

Up to now all this has been done manually which means a lot of routine work for archaeologists and a very inconsistent representation of the real object [15]. First, there may be errors in the measuring process, diameter or height may be inaccurate. Second, the drawing of the fragment should be in a consistent style, which is not possible since a drawing of an object without interpreting it is very hard to do. The third process, grouping or classifying, is also a very difficult task. There have been several attempts to develop a reliable method of classification [2, 16, 7, 4, 1, 21], none of which is widely accepted. A graphic documentation done by hand additionally raises the possibility of errors. This leads to a lack of objectivity in the documentation of the material found. To give an example, a vessel was drawn by four different illustrators resulting in four different vessels as shown in Figure 3. Note the different shape and decoration, the rim and the thickness for instance are significantly different.

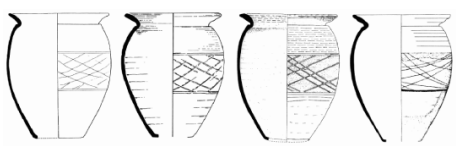

Figure 3: *The limits of objective recording: The same vessel drawn by four different illustrators (from [15]).*

2.1. Acquisition

At excavations most of the finds are in the form of fragments, with only a few still complete. It would be ideal to have one acquisition system that covers both sorts of objects, however, they do have different properties like dimensions, color, and geometry. Furthermore, the acquisition time for fragments has to be short. For complete vessels, since they are rare, the acquisition time is not critical but the output should be accurate in all dimensions.

The range and pictorial information of a fragment provided by the acquisition system is the basis for the further documentation and reconstruction process.

2.2. Orientation

The term *orientation* describes the exact position of a fragment on the original vessel. Finding the proper orientation of a fragment is one of the main tasks of the archaeological classification process [15]. The basis for classification and reconstruction is the profile. Hence the position of a fragment (orientation) on a vessel is important.

The manual process of making pottery with the potter's wheel is primarily based on the rotation of the potter's wheel and the forming through the potters own hands. The newly formed pot is built up vertically around the axis of rotation. The upper part of the vessel, which is called the rim, terminates in the so called orifice plane. Based on the orifice plane the archaeologist first orients the rim sherd according to its former position on the original vessel. If the fragment shows a section of the rim, the simplest way of manually establishing its orientation is by placing it upside down i.e. with the rim on a horizontal surface (see Figure 4).

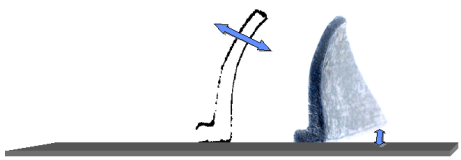

Figure 4: *Archaeological approach for finding the correct orientation of a rim fragment.*

Archaeologists use a horizontal surface like a ruler or a table etc. to orienta the fragment by aligning the fragment with the plane: they look for the position where a minimum gap exists between the plane of the rim fragment and the chosen horizontal plane. The gap is clearly shown by the amount of light coming through. Once the point of greatest resemblance is found, the measuring of the fragment, which consists of weighing and measuring the geometric form (i.e. height, width, area, etc.), is performed. Furthermore, the diameter is estimated. For fragments where the rim (the upper end of the vessel) is present, this is done by using a rim-chart. Figure 5 shows the measuring of a rim fragment.

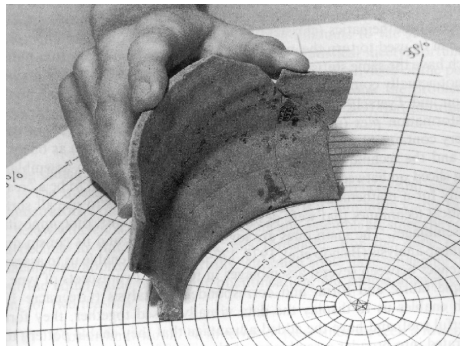

Figure 5: *Measuring the diameter using a rim chart (from* [15]*).*

For non-rim fragments the diameter of the original vessel is estimated in a similar way, but only if the size of the fragment is large enough.

3. Automatic Reconstruction

In order to automatically estimate the profile of a particular fragment, R. Halir proposed in [8] a multi-step approach based on a 3D model of a fragment. The estimation process starts with an estimation of an initial position of the rotation axis by a direct linear least squares optimization. Next a robust estimation is based on M-estimators. Finally an iterative refinement of the estimated axis is done by circle and line fitting methods. Pottmann et al. [18] proposed an algorithm to reconstruct surfaces of revolution using concepts from line geometry. Their approach is based on the fact that normals of these surfaces are given by linear equations in the Pluecker coordinates. Cao et al. [3] described an approach for finding the geometric structure of an axially symmetric pot. Their method is based on the fact that for each point of the surface, the center of the sphere of principal curvature corresponds to the circles of revolution is on the axis of revolution. By finding the line which minimizes the weighted least squares distance to the estimated centers, they find first the symmetric axis (orientation) and then the profile curve (profile extraction).

3.1. Orientation: Determination of the Axis of Rotation

In our approach the basis for this axis estimation is a dense range image provided by the range sensor. Our approach exploits the fact that surface normals of rotationally symmetric objects intersect their axis of rotation. The basis for this axis estimation is a dense range image provided by the range sensor. If we have an object of revolution, like an archaeological

vessel made on a rotation plate, we can suppose that all intersections n_i of the surface normals are positioned along the axis of symmetry a.
This assumption holds [8] for a complete object (Fig.5a) or even for its fragment (Fig. 5b). For each point on the object the surface normal has to be computed. A planar patch of size $s \times s$ can be fitted to the original data using the Minor Component Analysis [14], which minimizes the distance between the points of the surface and the planar patch in an iterative manner in order to compute the optimal value of the normal and discard outliers.
The axis of rotation a is determined using a Hough inspired method [23]. For each point on the object, the surface normals n_i are computed using Minor Component Analysis. In order to determine the axis of rotation a all surface normals n_i are clustered in a 3D Hough-space: All the points belonging to a line n_i are incremented in the accumulator. Hence the points belonging to a large number of lines (like the points along the axis) will have high counter values. All the points in the accumulator with a high counter value are defined as maxima.

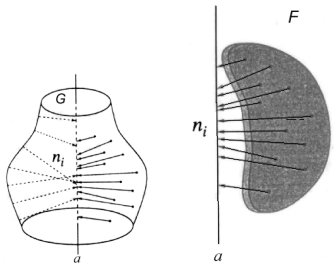

(a) (b)

Figure 6: *Surface normals n_i of a rotationally symmetric object O intersect the axis of rotation a; this should be true for complete objects (a) and for its fragments (b) (from [8])*

In the next step the line formed by the maxima has to be estimated. There are different techniques to solve this problem. The PCA or Principal Component Analysis [13] is a very popular method, which is used in our case. We have an a-priori knowledge: the maxima points are distributed according to a line (the axis of rotation). The PCA will determine the axis of maximal variance, which is in fact the axis of rotation. The accumulator maxima are taken as candidate points for the estimation of the axis of rotation. Using this technique outliers introduced by noisy range data or discretization errors, can be avoided, since in Hough-space incorrect data points are in the minority and do not build a maximum.

Figure 7 shows the result for a front-view of a fragment. On the left hand side of figure 7 the intensity image of the fragment is shown, on the right hand side the range image with the estimated rotational axis are depicted. A detailed description of the algorithm can be found in [10] and [20].

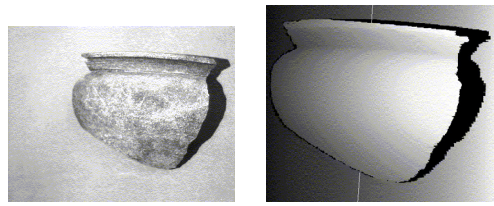

(a) (b)

Figure 7: *Intensity image (left) and range image (right) of a fragment with rotational axis of the front-view*

3.2. Profile extraction

Our algorithm for the estimation of the longest profile line consists of the following steps:

1. First the axis of rotation is transformed into the z-axis of the coordinate system in order to simplify further computation.
2. The fragment's size described by its circular arc is estimated. Depending on the size we compute a number of intersecting planes e_i, which are used for the profile estimation. The number of planes e_i depends on the length of the perimeter of the fragment. Experiments have shown that 7 to 13 profile lines return the best ratio of exactness and performance. Figure 8 shows a sample of 4 planes e_i intersecting the 3D-model and the plots of the extracted profile lines on the surface of the sherd.

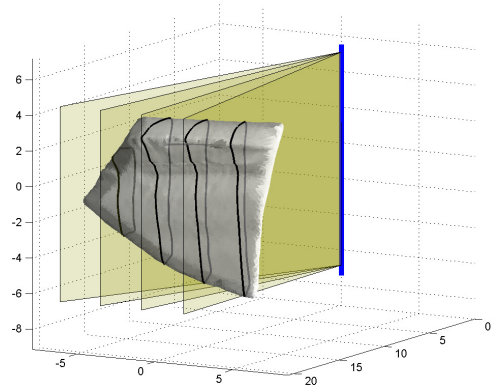

Figure 8: *Sample of intersecting planes e_i*

3. A profile line is calculated by intersecting the 3D-data of the fragment with planes e_i: First the distance of each vertex of the fragment to the plane e_i is calculated. All vertices are sorted by their distance to the plane. Then the nearest 1% of vertices are selected as candidates for the profile. For each of those vertices, all the patches to which they belong are filtered through a search in the patch list with their index number. In Figure 9 a sherd shaded by the value of distance to the intersecting plane is shown

(lighter means nearer to the intersecting plane). Every patch is a triangle which consists of three points that are connected by three lines. Every pair of vertices that has a point on both sides of the plane is part of the profile line, because its connection intersects the plane. The coordinates of these pairs are rotated into the xz-plane and the z-coordinate is removed. The result is a properly oriented profile line.

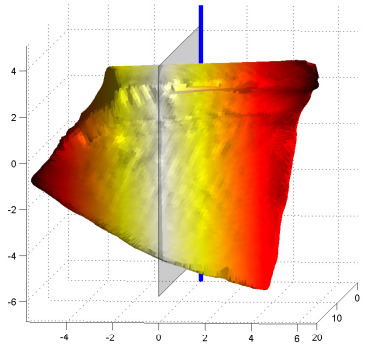

Figure 9: *Properly oriented sherd and intersecting plane e_i. The greyvalues corresponds to the distances. Lighter means nearer to the intersecting plane.*

4. Next the longest profile line is found: the difference between the maximum z-value and the minimum z-value of the profile line defines the height of the profile line. The remaining profile lines are used for evaluation of the estimate of the rotational axis.

4. Interactive Approach for Rim Fragments

We have designed a software tool to carry out the task of finding the correct orientation and profile for rim fragments in an interactive way. The software has been developed under Windows, using C++ as programming language and OpenGL as graphics library [5].

One of the aims of this software is that the archaeologist should feel comfortable working with it. Therefore, our system follows the same steps as in the traditional procedure, but introducing geometric and computational methods to minimize the errors of manual documentation.

4.1. Orientation

Orienting a rim fragment merely involves finding the orifice plane that contains the rim and rotating the sherd in such a way that the plane is parallel to the XZ plane.

This problem may be solved via Least Squares Fitting or other statistical or mathematical methods, but we have chosen a more flexible approach: Genetic Algorithms (GA) [12, 19]. This algorithms are easy to implement and allow the goodness criteria to be changed, it being possible to make the method more robust by adding constraints to the criteria (e.g. the incident axis of the surface normals).

Within our semi-automated approach the user interactively identifies the rim by selecting an area over the virtual sherd, making it possible to avoid irregularities of the rim. This selected area (shown in figure 10) is used for generating the population of the GA and finding the plane.

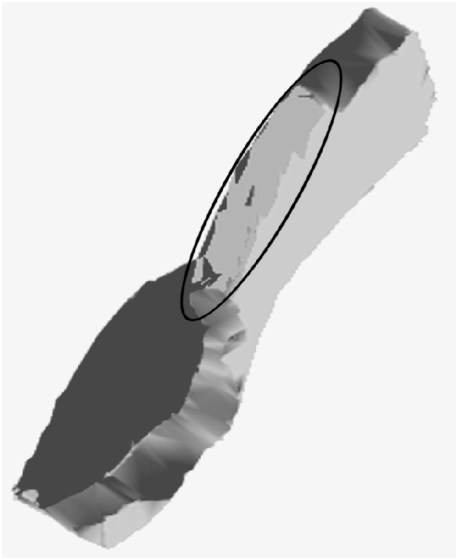

Figure 10: *Sherd with the relevant part of the rim marked (the area of interest is surrounded by an ellipse)*

A GA is based on a set of individuals, each one defined by a chromosome, which is a solution for the problem at hand. In our case, we have a chromosome composed of three genes, each one corresponding to a point of the selected rim. More precisely, the rim is divided into three zones (rightmost, central and leftmost) by a k-means algorithm, and the chromosome contains one gene for each zone. These three points define a plane, and our aim is to evaluate the goodness of this plane.

The goodness criteria for our chromosome (plane) is to consider the number of points of the rim contained by the plane and the number left to one side of the plane. That is to say, it is not sufficient to have a plane containing a lot of points, but it is also necessary for it to lean on the rim, just touching it, not crossing through the middle of the fragment. The goodness G of a chromosome c can be expressed as:

$$G_c = 100 \times \frac{|R_c - L_c|}{N_b} + P_c \qquad (1)$$

Where R_c and L_c are the number of points to the right and to the left respectively of the plane defined by c, and N_b is the

number of points selected as a part of the rim. P_c is the number of points whose distance to the plane is below a threshold ε.

The objective of our GA is to find the chromosome (plane) that maximizes this function. This is done by crossing and mutating individuals during a number of generations.

All parameters of the GA (e.g. crossover and mutation probability) can be modified by the user, leading to an improvement in robustness.

4.2. Diameter estimation

Estimating the diameter of the original vessel is analogous to finding the rotational axis of the pot. As we work mainly with prehistoric ceramic, made without a potter's wheel, its surfaces are very irregular, and it is not easy to find the axis by calculating the incident axis of the surface normals [8].

We use a procedure similar to the traditional one:

- By moving a horizontal plane, the expert selects a section of the sherd (Figure 11). This section is an arc, and so the expert might have selected the longest arc or the one with the fewest irregularities.
- Having this arc (in fact, it is a double arc: the external and the internal), the problem is now that of finding the center of the circle that best fits the external arc.

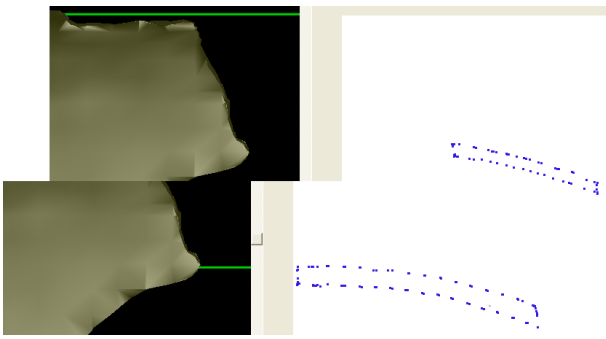

Figure 11: *Two arcs obtained at different heights of the sherd by intersecting it with a horizontal plane.*

To fit the circle to the arcs, we follow a LSQ fitting algorithm. First, we fit a circle using both arcs, so it will pass between them. Then, we remove the internal points and repeat the procedure with the external ones, so the new circle fits by minimizing the geometric distance with the sequence of points that define the external arc. The rotational axis is the vertical line that passes through the center of the calculated circumference.

4.3. Profile extraction

From the 3D model of the sherd, the expert selects those areas considered as best defining the shape of the profile. This step is done by drawing lines over the sherd, using the mouse, as if it were a pen over the real sherd (Figure 12). We obtain a set of 3D lines that are projected over the planes containing the previously calculated rotational axis. This can be done because we have previously translated the point coordinates into polar coordinates; when selecting a point, we take the modulus and the azimuth of its polar coordinate, and so it is easily translated into 2D coordinates.

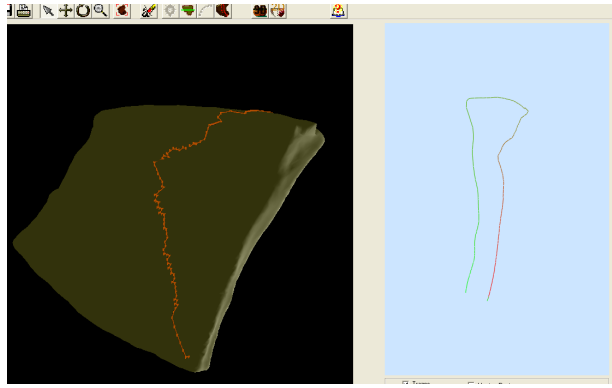

Figure 12: *Profile extraction: the strokes on the left image indicate the profile obtained.*

Given the sequence of 2D lines, the system fixes them in a unique stroke, detecting overlappings and irregularities. This profile is fully editable, it being possible to add, eliminate or move points, e.g. if the software does not remove all irregularities, the expert can do it in a few seconds. A detailed description of the algorithm can be found in [11]

The drawing of the vessel includes an estimated profile that indicates how the profile would have continued if the whole vessel had been available. The length of this estimation differs from one sherd to another, because it depends on the typology and the experience of the expert, but standard practice is to extend it by about two centimetres.

The software generates a first approach to this prolongation by a cubic spline that follows the shape indicated by the lowest 15% part of the profile. This spline is calculated by taking 4 points separated by 5% of the height of the profile obtained. As typologies in prehistoric ceramics are very hard to establish, and very restricted to small areas, we consider that the experience of the expert is very important at this point, so we also allow him/her to edit the estimated prolongation, by moving the points or the tangents at the end of the prolongation (See Figure13).

5. Results

Based on the approach presented in Section 3 we illustrate three reconstructed profiles which thereby represent further profile reconstructions from our pottery dataset. The x- and y axis denote the diameter and the height ($y = 0$ in the middle)

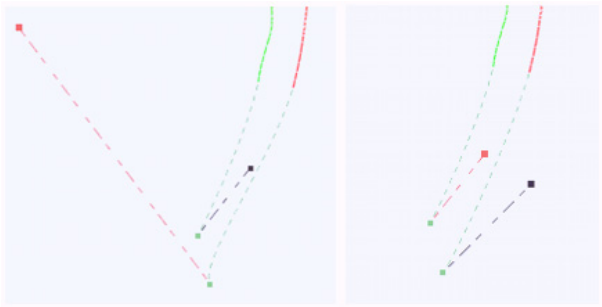

Figure 13: *Editing the estimated profile: Note the tangent has been moved and the stroke has changed.*

of the fragment respectively. The area between the inner and outer profile is drawn black in order to have a similar representations as manual drawings. This automatically generated drawing is intended for use in archaeological publications.

Figure 14a shows the profile of fragment 1 from box 2 (Figure 14b) with an average inner diameter of 9.56 and an average outer diameter of 10.38. The computed average thickness is 0.81cm. The average height of the fragment is 6.5cm. The profile represents a wall fragment, which is indicated by the straight ending at the top of the profile.

(a) (b)

Figure 14: *(a) reconstructed profile section and (b) Image of fragment 1 from box 2.*

Figure 15a shows the profile of fragment 6 from box 2 (Figure 15b) with an average inner diameter of 2.01 and an average outer diameter of 3.04. The computed average thickness is 1.03cm. The average height of the fragment is 10.06cm. The profile represents a rim fragment, which is indicated by the curved ending at the top of the profile.

Figure 16a shows the profile of fragment 8 from box 1 (Figure 16b) with an average inner diameter of 10.97 and an average outer diameter of 15.58. The computed average thickness is 0.39cm. The average height of the fragment is 5.1cm. The profile represents a wall fragment, which is indicated by the straight ending at the top of the profile.

(a) (b)

Figure 15: *(a) Reconstructed profile section and (b) Image of fragment 6 from box 2*

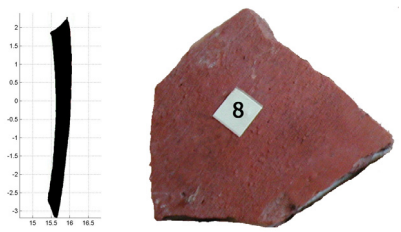

(a) (b)

Figure 16: *(a) Reconstructed profile section and (b) Image of fragment 8 from box 1*

The resulting 3D reconstruction of fragments depends on the correct orientation of the profile section. The evaluation of the 3D representation is rather complicated since ground truth is not available due to the fact that there is no 3rd dimension in archaeological archive drawings and the object does not exist in reality. The description of shape is subject to the ideas of the archaeologists and is not standardized.

Experiments were done on all 40 fragments of our pottery database. The success rate for correct extraction of the profile line and consequently the percentage of sherds used for further reconstruction is around 50% of the data found at the excavation site. This should be compared to manual archivation done by archaeologists [15]: for coarse ware around 35% [6] and for fine ware around 50% [17] of the findings are used for further classification. It heavily depends on the shape of the fragment (e.g. handle, flat fragments like bottom pieces, small size, etc.). 18 fragments have been excluded from reconstruction due to incorrect estimation of the axis of rotation.

Table 1 summarizes the results for 22 properly orientated fragments. Box and piece numbers are used for identification of the fragment. The radius r is the estimated mean radius of the profile line. The standard deviation of the radius was estimated along the perimeter of the fragment. The thickness of the fragment is the difference between the mean radius of the inner side and the outer side. The fragment size is the percentage of the perimeter of the sherd compared to the perimeter of the whole object.

Box Nr.	Sherd Nr.	Radius (*cm*)	Std. dev. (*cm*)	Mean thickness (*cm*)	Fragment size (%)
1	04	10,20	0,05	0,51	11,13
1	08	15,78	0,04	0,39	4,78
1	16	14,56	0,09	1,75	6,36
1	17	16,15	0,15	1,51	8,08
1	18	15,16	0,03	1,75	5,12
1	19	14,54	0,15	0,84	8,25
1	20	12,99	0,08	1,56	7,55
1	22	11,53	0,10	0,75	13,55
1	23	12,33	0,08	0,65	8,72
2	01	9,97	0,09	0,82	11,15
2	02	15,95	0,03	1,13	6,35
2	04	6,66	0,18	1,67	17,03
2	05	9,94	0,08	0,49	8,94
2	06	2,35	0,21	1,03	31,51
2	09	12,3	0,08	0,97	9,06
2	10	18,33	0,06	1,00	5,91
2	11	10,2	0,05	2,24	9,09
2	12	12,34	0,12	0,982	10,04
2	14	16,91	0,17	1,52	12,61
2	15	15,42	0,07	1,21	8,4
2	16	14,36	0,12	1,53	8,47
2	18	10.8	0,06	1,93	9,69

Table 1: *Results for 22 fragments*

Experiments with synthetic data have shown that the correctness of the reconstruction depends on the correct estimation of the axis of rotation (see [20] for a detailed survey) and on the resolution of the 3D scanner used. The number of vertices in the data used ranges between 4000 and 15000, leading to a profile line with 200 to 300 points. The execution time using a prototype written in Matlab running on a *Pentium III* 1 GHz is less than a minute per sherd. It depends heavily on the computation of the axis of rotation (70% to 80% of the execution time).

In order to demonstrate the correctness of the computed profile lines, Figure 17 shows a recorded sherd (dark object) and its computed profile section (vertical line). The computation of the virtual fragment (grey object) is based on the profile section. One can see that the recorded fragment fits into the virtual fragment, which indicates that the computation is correct. Following multiple cross-sections along the perimeter of the virtual fragment one can see hardly any deviation from the original fragment. Some deviations are caused by the bumpiness of the surface, as the surface is not exactly rotationally symmetric since it is hand-made pottery.

If the fragment was orientated incorrectly, the recorded fragment does not fit into the virtual object and multiple

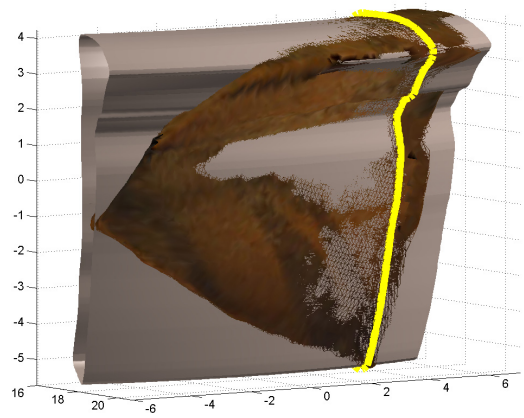

Figure 17: *Reconstructed fragment, profile section and recorded fragment*

cross-sections along the perimeter of the virtual fragment show large deviations from the original object.

Following the approach described in Section 4, the traditional drawing of the ceramic is obtained, after the profile and the rotational axis have been computed (see Figure 18).

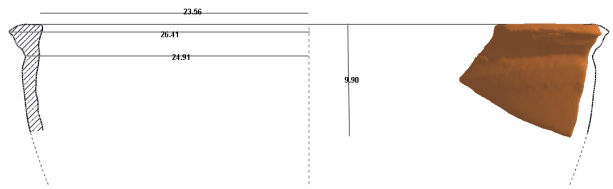

Figure 18: *2D drawing of the computed profile following the archaeological standards*

This step of the reconstruction process is also interactive, because the system allows the expert to:

- Choose the position of the sherd in the drawing, depending on the details he wants to show. As in manual drawings, a false perspective is used, to avoid hiding part of the surface when placing the sherd at the left or rightmost position.
- Modify the lighting, to improve the visualization of several details of the sherd.
- Take measurements over the drawing, such as the diameter at several points, height of the sherd, etc... This measurements can be translated, modified, etc...

This image can be saved as a BMP, GIF or JPEG image, and so it can be edited by any image editing software.

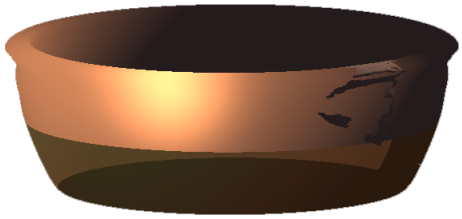

Figure 19: *Virtual 3D Reconstruction of Vessel*

The 3D reconstruction of the pot is generated by rotating the profile (both the real one and the estimated prolongation) around the rotational axis. The surface corresponding to the estimated part of the pot is shown with a semi-transparent texture, in order to identify clearly both parts of the reconstruction. The original sherd is shown in the vessel, as in real reconstructions, so the quality of the reconstruction and the exact place where it was located can be seen (Figure 19). The reconstruction can be rotated and zoomed to obtain different views of the vessel, each view can be saved as an image.

6. Conclusions

We have proposed two approaches for the computer aided reconstruction of archaeological fragments. Both methods have in common that they compute the axis of rotation of archaeological fragments in order to find the correct orientation. With the help of the axis of rotation a profile line is extracted and a vessel is reconstructed. The Hough-inspired approach works independently from the orifice plane, consequently it is possible to reconstruct vessels out of bottom- or wall fragments as well. It is fully automated. The GA-based method works on rim-fragments only, allowing the user to adjust the results step-by-step. This semi-automated approach is very useful for hand-made or irregular -with respect to its radial symmetry- fragments, because the user may correct the position of the axis, in order to fulfill his expectation as an expert.

At the profile extraction step, the automatic approach uses the longest profile, whereas the interactive approach allows the user to select those areas on the sherd, which he or she thinks are a reliable representation of the fragment. For example in the automated approach, the handle or the decoration of a fragment could lead to an incorrect profile line, because the longest profile could include parts of the decoration or simply an irregular surface (see Figure 20). Consequently at this point the interactive approach offers more robustness.

The Hough-inspired approach allows automatic classification, so the archaeologist gets the typology in a few seconds. Furthermore the computed typology is used to find matching fragments of the same vessel. A fully automated system for the documentation of archaeological fragments allows the processing of large dataset in reasonable time (1 fragment per minute).

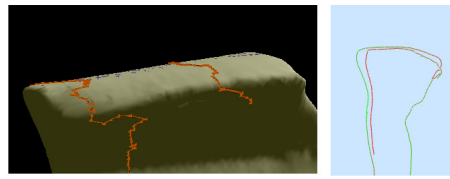

Figure 20: *Selecting distinct areas of the rim (left) allows two different profiles to be obtained*

The GA-based approach offers a drawing tool, which allows archaeologists to easily obtain graphical documents for their publications. They may apply their standards in a faster and more accurate way, then doing it manually. The interactivity on the design of the final drawing is a powerful characteristic, because it allows the user to generate different drawings of the same pot by simply moving the sherd, changing the lightning or showing different measurements.

The two approaches presented are not in conflict with one another, but can be considered as complementary. As an outlook for further research we plan to develop a combined system that covers the two approaches in order to overcome the weaknesses of each algorithm and to combine the benefits, leading to a powerful instrument, which serves the need of the archaeological community.

7. Acknowledgements

This work was partly supported by the Spanish Ministry of Science and Technology (MCYT) under project TIC2001-2099-C03-02, the Austrian Science Foundation (FWF) under grant P13385-INF, the EU under grant IST-1999-20273 and the Austrian Federal Ministry of Education, Science and Culture.

References

1. W. Adams and E. Adams, *Archaeological Typology and Practical Reality. A Dialectical Approach to Artifact Classification and Sorting*. Cambridge, 1991.
2. L. Binford, "Archaeological Systematics and the Study of Cultural Process," *American Antiquity*, vol. 31, pp. 203–210, 1965.
3. Y. Cao and D. Mumford, "Geometric structure estimation of axially symmetric pots fromsmall fragments," in *Signal Processing, Pattern Recognition and Applications*.
4. W. Czysz and W. Endres, *Archäologie und Geschichte der Keramik in Schwaben*. Neusädt, 1991.

5. T. Davis, J. Neider, and M. Woo, *OpenGL Programming Guide*. Addison-Wesley, 1993.

6. R. Degeest, "The Common Wares of Sagalassos," in *Studies in Eastern Mediterranean Archaeology*, ser. III, M. Walkens, Ed., 2000.

7. W. Erdmann, H. Kühn, and H. Lüdtke, "Rahmenterminologie zur mittelalterlichen Keramik," 1984.

8. R. Halíř, "Estimation of Rotation of Fragments of Archaeological Pottery," in *Proc. of the 21st Workshop of the Austrian Association for Pattern Recognition (ÖAGM)*, W. Burger and M. Burge, Eds., Hallstatt, Austria, May 1997, pp. 175–184.

9. J. W. Hayes, "Recent Work on Roman Imported and Local Pottery from the Athenian Agora and the Isthmian Sanctuary," in *Hellenistische und kaiserzeitliche Keramik des östlichen Mittelmeergebietes, Kolloquium Frankfurt*, 1995, pp. 7–17.

10. M. Kampel and R. Sablatnig, "An automated pottery archival and reconstruction system," *Journal of Visualization and Computer Animation*, vol. 14, no. 3, pp. 111–120, July 2003.

11. F. Melero, J. Torres, and A. León, "On the interactive 3d reconstruction of iberian vessels," in *Proc. of the 4th Int. Symposium on Virtual Reality, Archaeology and Intelligent Cultural Heritage*, D. Arnold, A. Chalmers, and F. Niccolucci, Eds., Brighton, November 2003.

12. Z. Michalewicz, *Genetic Algorithms + Data Structures=Evolution Programs*. Springer Verlag, 1996.

13. E. Oja, *Subspace Methods of Pattern Recognition*. John Wiley, 1983.

14. E. Oja, L. Xu, and C. Suen, "Modified Hebian Learning for Curve and Surface Fitting," *Neural Networks*, vol. 5, no. 3, pp. 441–457, 1992.

15. C. Orton, P. Tyers, and A. Vince, *Pottery in archaeology*. Cambridge: Cambridge University Press, 1993.

16. H. Petrikovits, "Taxonomie und Beschreibung römischer Gefäßkeramik," in *Novaesium V. Die römische Keramik aus dem Militärbereich von Novaesium, Limesforschungen 11*, Berlin, 1972.

17. J. Poblome, "Sagalassos Red Slip Ware," in *Studies in Eastern Mediterranean Archaeology*, ser. II, M. Walkens, Ed. Brepols, 1999.

18. H. Pottmann, M. Peternell, and B. Ravnani, "An introduction to line geometry with applications," in *Computer Aided Design*, ser. 31, 1999, pp. 3–16.

19. C. Reynoso and E. Jezierski, "Genetic algorithm solver for archaeology," in *29th Conference of CAA: Pushing the Envelope*, ser. BAR International Series, G. Burenhult and J. Arvidsson, Eds., no. 1016, Gotland, Sweden, April 2001.

20. R. Sablatnig and M. Kampel, "Model-based registration of front- and backviews," *Computer Vision and Image Understanding*, vol. 87, no. 1–3, pp. 90–103, July 2002.

21. C. Sinopoli, *Approaches to Archaeological Ceramics*. New York, 1991.

22. C. Steckner, "SAMOS: Dokumentation, Vermessung, Bestimmung und Rekonstruktion von Keramik," *Akten des 13. internationalen Kongresses für klassische Archäologie - Berlin*, pp. 631–635, 1988.

23. S. B. Yacoub and C. Menard, "Robust Axis Determination for Rotational Symmetric Objects out of Range data," in *21 th Workshop of the Oeagm*, W. Burger and M. Burge, Eds., Hallstatt, Austria, May 1997, pp. 197–202.